Effects of Pre-insertion Resistor on Energization of MMC-HVDC Stations

Lina He, *Member, IEEE*

***Abstract*—With the development of power electronics technology, the modular multilevel converter (MMC) based HVDC has become one of the optimal solutions for large-scale renewable energy integration and network interconnections. When a MMC-HVDC station is in the status of energization, all the controllable switches in the MMC converter need to be switched off. It makes the converter become a three-phase uncontrollable diode bridge. Its electromagnetic transient model has been proposed in this paper. In addition, the generic model of a MMC-HVDC station has been developed on the Siemens PTI software PSS®NETOMAC, in order to study the energization transients of a MMC-HVDC station, say, Siemens HVDC PLUS. The simulation results show that the pre-insertion resistor (PIR) can effectively suppress inrush currents of the converter transformer, and alleviate the effects of converter harmonics on the HVDC-connected network. In the energization circuit, the PIR is bypassed after a selected insertion time, usually a few seconds. The resulting transient current involves a dc component that can result in current zero-crossing missing phenomena and endanger security of power system devices. Therefore, it is significant to determine an appropriate PIR to avoid dangerous inrush currents and possible current zero-crossing missing issues.**

***Index Terms*—MMC-HVDC, energization, PIR, transformer saturation, inrush currents, converter harmonics, current zero-crossing missing.**

I. Introduction

DURING the last decade, the penetration of renewable energy, including offshore wind power, has been dramatically integrated with ac mainland grids to achieve an overall reduction of green house gas emissions. A report from European Wind Energy Association (EWEA) has shown their ambition to increase the installation capacity of offshore wind units to 150 GW by 2030 that is going to meet 14% of the European electricity demand [1-3].

However, the rapid growth of offshore wind power raises new technical challenges. Due to its inherent characteristics of large scale and long distances, the MMC-HVDC technology has become one of the optimal solutions for offshore wind power integration. Its typical advantages include fast and independent control of active and reactive power, feasibility of multi-terminal dc grids, black start capability, and so on. Currently, a couple of MMC-HVDC connections have been installed in European water to deliver offshore wind power to onshore ac grids. For example, the MMC-HVDC connection called BorWin2, links the Global Tech 1 offshore wind farm in the North Sea to mainland Germany via a dc cable connection with a length of 200 km [4].

A MMC-HVDC station usually consists of a power converter, a transformer, and a circuit breaker (CB) with a PIR. When a MMC station is energized by switching on the CB on the HVDC feeder, the resulting abrupt voltage change can lead to the saturation of the transformer core. Due to the magnetizing characteristic, the magnetizing impedance of the transformer is significantly reduced after its saturation. The caused inrush current on the primary side of the transformer can be up to several times of its rated current. As a result, the point of common coupling (PCC) of the HVDC experiences a dramatic voltage dip that can induce severe distortions on voltage and current waveforms of the HVDC-connected network. The possibly caused overcurrents and overvoltages can active the malfunction of protective devices in extreme situations.

During the energization of a MMC-HVDC station, the power converter is required to be blocked. That is, the power semiconductors with turn-off capability, such as insulated gate bipolar transistors (IGBTs), need to be switched off. It makes the MMC converter become an uncontrollable diode bridge. In this circuit, the switching operations of the diodes depend on the instantaneous voltages at the ac side of the converter. The caused natural diode switching behavior generates unexpected lower-order harmonics. Differing from the two or three-level voltage source converter (VSC) based HVDC, the MMC-HVDC station is not equipped with an ac filter. Therefore, the generated lower-order harmonics cannot be eliminated. The caused waveform distortions by the harmonics can impact the power quality of the connected ac network. In addition, these lower-order harmonics could intensify the saturation of the converter transformer, leading to more severe inrush currents.

In order to counteract the accompanied dangerous transients during energization, the PIR is usually installed in the MMC-HVDC station. However, the detailed effects of the PIR during energization have not been discussed in the existing literatures yet, to the best of author's knowledge. Only a couple studies have investigated the energization performance of the two or three-level VSC-HVDC. For example, the work in [5] discussed the energization transient performance of the VSC-HVDC network based on the two /three-level technology.

With large-scale power electronics interfaced renewable energy integration, the resulting impact on power system switching transients, e.g., energization transients, has become a new challenge that needs to be addressed to ensure security

Lina He is with Siemens PTI, (e-mail: lina.he@siemens.com).

978-1-5386-2212-4/17/$31.00 ©2017 IEEE

of power system devices. This paper focuses on the energization of a MMC-HVDC station to study its transient performance and corresponding impacts on the connected network.

The structure of this paper is as follows. The electromagnetic transient model of the MMC converter during energization is proposed in Section II. Based on the proposed converter model, Section III develops the generic model of a MMC-HVDC station on the Siemens PTI software PSS®NETOMAC to study its energization transients. Regarding the generated inrush currents and voltage dips, the PIR is applied as a mitigation method during energization. The simulation cases with and without a PIR are demonstrated in Section IV to evaluate the effects of the PIR on the energization of a MMC-HVDC station. Section V concludes.

II. Electromagnetic Transient Model of MMC Converter during Energization

The MMC technology has been introduced by Siemens to the HVDC applications, so called HVDC PLUS. The configuration of a half-bridge MMC is shown in Fig. 1 (a). As seen, it consists of a three-phase bridge, where each of the six converter arms is formed by a number of identical but individually controllable submodules (SMs) and a reactor. Each submodule contains an IGBT half bridge as a switching element and a capacitor unit for energy storage, as shown in Fig. 1 (b) [6][7]. This submodule can be operated in three different states, including capacitor-on, capacitor-off and energization.

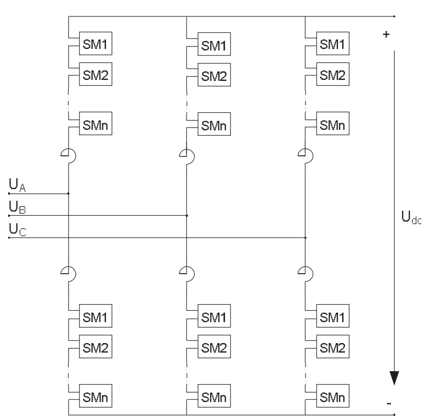

(a)

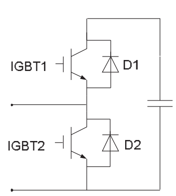

(b)

Fig. 1 (a) MMC configuration, and (b) submodule of MMC

In the state of capacitor-on, the voltage of storage capacitor in Fig. 1 (b) is applied to the terminals of the submodule. Depending on the flow direction, the current circulates either through D1 to charge the capacitor, or through IGBT1 to discharge the capacitor. For the status of capacitor-off, the current flows through IGBT2 or D2 that makes the voltage crossing the submodule terminals be zero. In this situation, the capacitor voltage remains unchanged. During the operation of MMC-HVDC, each submodule in a converter arm is individually selected and controlled. With the appropriate control strategy, the MMC can provide a fine gradation of the output voltage. The more steps are used, the proportion of harmonics is smaller and the high-frequency noise is lower. Thus, each converter arm can be represented as a controllable voltage source if it consists of enough submodules. By adjusting the ratio of the converter arm voltages in each phase, the desired sinusoidal voltage at the ac terminal is able to be achieved. Therefore, it is not negligible to equip an ac filter with the MMC converter.

During the energization of a MMC station, both IGBTs in each submodule are switched off. When the CB on the HVDC feeder is switched on for energization, the current flows from the ac terminal to the positive dc pole to charge the capacitor. If the current flows in the opposite direction, the freewheeling diode D2 bypasses the capacitor. As a result, the converter circuit during the status of energization becomes a diode bridge. The voltages of converter arms cannot be controlled any more. By aggregating all the submodules in each converter arm, the electromagnetic transient model of the MMC converter can be represented in Fig. 2. It is seen that the MMC converter behaves as a three-phase uncontrollable diode bridge during its energization. The generated harmonics during operation can result in a high total harmonic distortion (THD) at the connected network.

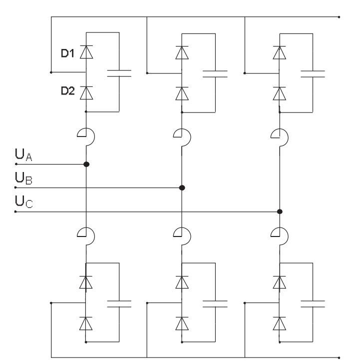

Fig. 2 Electromagnetic transient model of MMC during energization

III. Generic Model for Energization

A generic model is developed in this section to analyze the energization transients of a MMC station. Its configuration is shown in Fig. 3. In this model, the network is represented by a Thevenin equivalent circuit. Via a CB, it is connected to an ac cable/OHL that is modeled as a series-connected Pi circuit. Each Pi circuit corresponds to a segment of the transmission line with a short length. The PIR is usually installed at the MMC station to avoid high inrush currents and severe voltage dips at the PCC. It is noted that the CB1 with a PIR is located between the converter transformer and the power converter

978-1-5386-2212-4/17/$31.00 ©2017 IEEE

according to the Siemens HVDC PLUS technology.

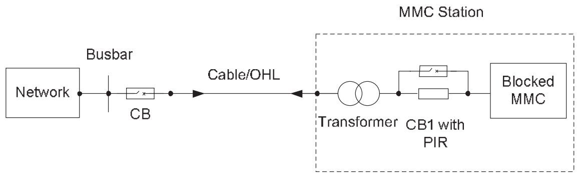

Fig. 3 Generic model of MMC station for energization

A. Transformer Modeling

The transformer consists of two parts, i.e., the iron core and windings. Since the studied energization transients are in the range of low/mid-frequency, the transformer can be represented by a lumped parameter model [8]. Its single phase model is shown in Fig. 4. As seen, this model applies a R-L circuit to ensure the appropriate frequency response of the transformer. The saturation characteristic of the core is included in the magnetizing branch.

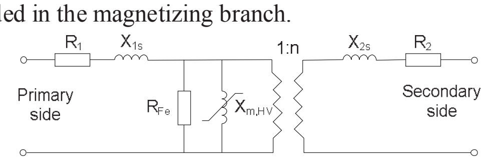

Fig. 4 Single phase model of transformer

The symbols $\mathrm{R_1}$ and $\mathrm{X_{1s}}$ correspond to the primary winding resistance and leakage reactance in the primary side, respectively. The magnetizing branch is composed of the core resistance $\mathrm{R_{Fe}}$ and magnetizing reactance $\mathrm{X_m}$. In the secondary side, the symbols $\mathrm{R_2}$ and $\mathrm{X_{2s}}$ indicates the secondary resistance and leakage reactance in that side, respectively. In this T-equivalent model, the saturation characteristic is modeled as a simplified two-slope piecewise linear function. The detailed relationship between the crossing voltage and flowing current of the magnetizing branch is shown in Fig. 5.

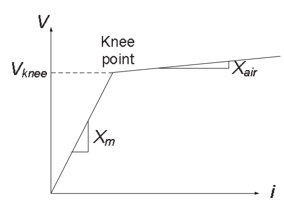

Fig. 5 Simplified two-slope magnetizing characteristic

It is seen in Fig. 5 that the slope of the line is equal to the magnetizing reactance $\mathrm{X_m}$ when the transformer voltage is under the saturation knee point V_{knee}. When the CB on the HVDC feeder is switched on to energize the MMC station, the sudden voltage change is added to the converter transformer. As a result, the flux in the transformer core will be dramatically increased due to the relationship between the flux and voltage shown below,

$$V = d\psi/dt \tag{1}$$

The maximum theoretical value of this flux can be up to two to three times of the rated flux peak. Due to the magnetizing characteristic, the magnetizing reactance is dramatically reduced to the air-core reactance $\mathrm{X_{air}}$. Thus an inrush current occurs. Besides the voltage added to the transformer, the remanent flux also has a significant impact on the inrush current. The remanence is the magnetization remaining in the transformer iron core after the transformer is switched off last time. Its maximum amplitude is usually in the range of 0.6-0.8 p.u.. It can force the iron core to get into saturation soon when this transformer is switched on again.

B. CB with PIR in MMC Station

The model of the CB with a PIR is illustrated in Fig. 6. As seen, the PIR is in parallel with the CB1. A switch s1 is applied to control the connection of the PIR. Before the MMC converter started to be energized, the switch s1 is closed to insert the PIR. It helps to damp possible overvoltages and overcurrents during energization. After a selected insertion time (usually a few seconds), the CB1 is switched on to bypass the PIR. The status of the switch s1 is not changed after the CB1 is switched on, i.e., the PIR remains connected during operation.

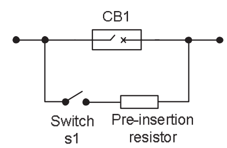

Fig. 6 Model of CB with a PIR

IV. CASE STUDY

A. Simulation Data

The generic model of a MMC station during energization is developed on the Siemens PTI software PSS®NETOMAC (Version 11.5) for time-domain simulation. The applied parameters are provided by a TSO, including the network, cable, converter transformer, PIR and MMC converter. The corresponding details are listed in Appendix. The length of the cable is 0.671 km. Its resistance, reactance and capacitance per km are 0.037 Ohm, 0.11 Ohm and 230 nF, respectively. Here, the three-winding converter transformer is simplified to a two-winding transformer. This simplification does not impact the accuracy of the simulation results, since the capacity of the tertiary winding is very small, only 3 MVA.

The studied grid is operated at a nominal voltage of 400 kV with a rated frequency of 50 Hz. As discussed in Section III, the transmission line is modeled as a series-connected Pi circuit. Each Pi circuit in the simulation model corresponds to a transmission line with a length of 30 m. According to the transformer parameters, the corresponding magnetizing characteristic curve is modeled on PSS®NETOMAC. In the simulation, the highest remanence of 0.8 p.u. is applied to perform the worst cases. For the blocked converter, the inductance and the aggregated capacitance in the each converter arm correspond to 53.9 mH and 50 µF, respectively.

B. Simulation Results

This section is aimed to investigate the impact of the PIR on the energization of a MMC-HVDC station. The simulation results with and without a PIR are described below, respectively.

In the simulation cases, the remanence flux of the converter transformer in phase A is assumed with the highest amplitude of -0.8 p.u.. It can be calculated that the corresponding remanence fluxes in phases B and C are 0.4 p.u.. Based on the relationship between the transformer voltage and flux as described in (1), the caused inrush current in a single phase system is with the maximum amplitude when the corresponding CB pole is switched on at a zero-crossing of its phase-to-ground voltage. This switching strategy is applied in the simulation cases to perform the worst cases. It is noted that a pole switching device (PSD) is not considered for the CB on the HVDC feeder. Therefore, the switching time of each CB pole cannot be controlled independently.

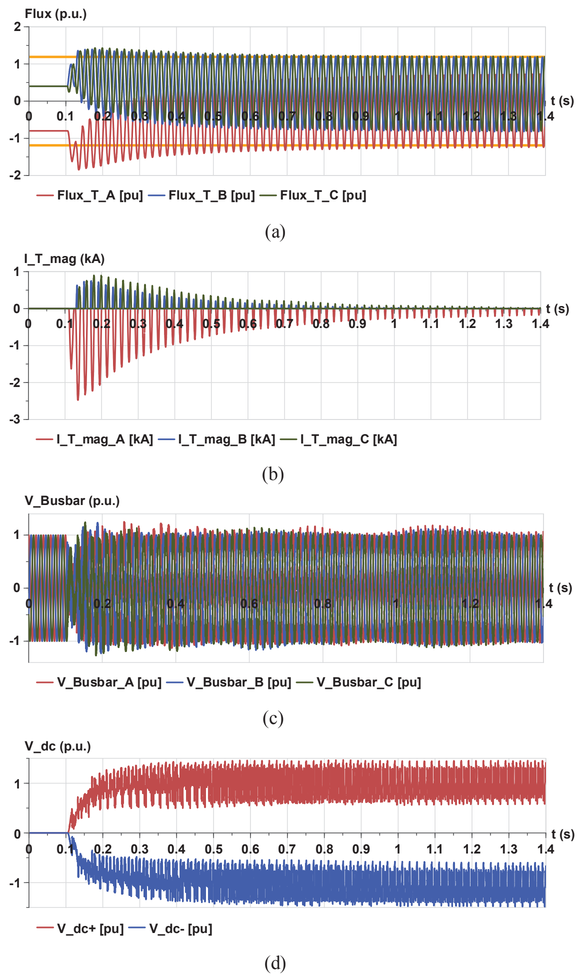

Fig. 7 Simulation results without a PIR: (a) flux of converter transformer; (b) inrush currents flowing through magnetizing branch of transformer; (c) busbar voltage; (d) dc side voltages of converter.

Without consideration of the PIR, the CB is switched on at a zero-crossing of the phase A-to-ground voltage, i.e., 0.1 s, to energize the converter station. The resulting abrupt voltage change added to the transformer leads to the saturation of the transformer core after about one cycle, as seen in Fig. 7 (a). The shown orange horizontal lines indicate the saturation limit 1.195 p.u. of the converter transformer. Based on the magnetizing characteristic as discussed in Fig. 5, the magnetizing impedance of the transformer is reduced dramatically to its air-core impedance after the transformer saturation. As a result, an inrush current is caused on the primary side of the transformer, as shown in Fig. 7 (b). That results in a significant voltage dip on the HVDC PCC point in Fig. 7 (c). It is noted that the CB1 is kept to be closed for bypassing the PIR in this case. Since the PIR is not connected, the converter energization is completed rapidly and the dc voltage reaches 1 p.u. after about 0.25 s. The corresponding simulation result is shown in Fig. 7 (d).

As seen in Fig. 7 (a), the fluxes in phases A, B and C are dramatically increased after the CB is switched on. All the three phases of the transformer get saturated rapidly. At 0.136 s, the flux in phase A is with the highest amplitude of 1.85 p.u. that is much higher than the saturation limit. As a result, an inrush current with the highest amplitude of 2.45 kA flows through the phase A of the magnetizing branch, as shown in Fig. 7 (b). The resulting voltage dip in phase A of the busbar is up to 0.6 p.u.. It is found in Fig. 7 (d) that the converter energization is completed rapidly and the voltages at dc+/- poles rise to 1 p.u. at about 0.35 s. After that, the voltage distortions at the busbar still appear, as shown in Fig. 7 (c). This is due to the harmonics generated by the blocked converter during energization.

In order to suppress the inrush currents, the PIR with the resistance of 1000 ohm is applied during the energization of the HVDC station. As noted, the PIR is connected to the circuit before the CB is switched on. Identical with the previous case, the CB is switched on to energize the MMC-HVDC station at 0.1 s. The corresponding simulation results are reported in Fig. 8. It is seen in Fig. 8 (a) that only the flux in phase A slightly beyonds the saturation limit of 1.195 p.u.. The resulting highest inrush current in this phase is about 0.052 kA. As shown in Fig. 8 (c), there is no obvious voltage dips at the busbar. Due to the high resistance of the PIR, the converter takes much longer time to complete its energization than that without a PIR. According to Fig. 8 (c), the busbar voltage curves do not have obvious distortions in the case with a PIR.

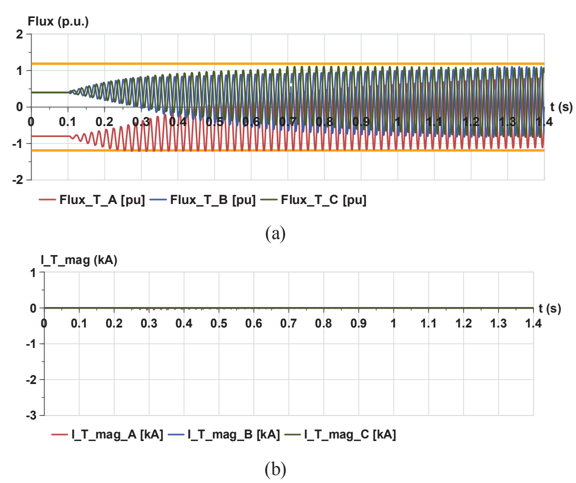

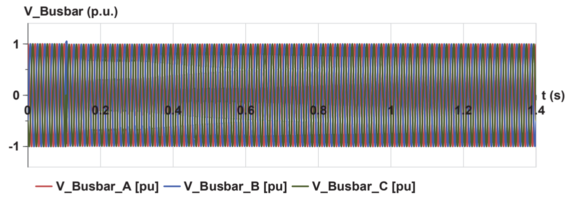

(c)

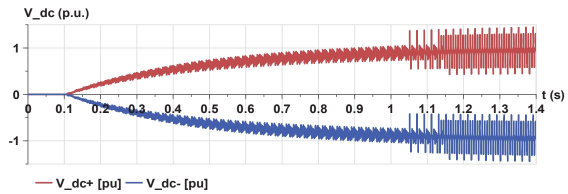

(d)

Fig. 8 Simulation results with a PIR: (a) flux of converter transformer; (b) inrush currents flowing through magnetizing branch of transformer; (c) busbar voltage; (d) dc side voltages of converter.

It is found that the PIR can effectively decrease the inrush currents and alleviate the impact of the converter harmonics on the HVDC-connected network. The insertion time of the PIR during the HVDC station energization is usually about several seconds. After the selected insertion time, the PIR is bypassed by switching on the paralleled CB1. At the mean time, a dc component current is generated simultaneously to maintain the current continuity. The amplitude of this dc component depends on the resistance of the PIR. The higher resistance of the PIR corresponds to the larger amplitude of the dc component. This dc component can result in zero-crossing missing phenomena. The relevant details have been described in [9]. Thus, the selection of the PIR in a MMC-HVDC station is significant.

V. Conclusion

During energization, the MMC converter behaves as a three-phase uncontrollable diode bridge. The corresponding electromagnetic transient model has been proposed in this paper. In order to investigate the energization transients of a MMC-HVDC station, say, Siemens HVDC PLUS, the corresponding generic model has been developed on the Siemens PTI software PSS®NETOMAC. The simulation cases analyze the inrush currents and voltage dips at the PCC during energization with and without a PIR. Based on the results, the PIR can effectively suppress transformer inrush currents and alleviate the effect of converter harmonics on the HVDC-connected network. When the PIR is bypassed by switching on the paralleled CB, the abrupt circuit change generates a dc component current that can cause current zero-crossing missing issues and endanger power system device security. Therefore, it is significant to determine an appropriate PIR in each HVDC PLUS project to avoid dangerous transformer inrush currents and possible current zero-crossing missing phenomena. In the future, the simulation results will be compared with the realistic measurements from an actual MMC-HVDC device to validate the accuracy of the proposed electromagnetic transient model.

Appendix

Table I
Parameters of Network

Symbols	Values	Units	Descriptions
V_r	400	kV	Rated voltage
f_r	50	Hz	Rated frequency
I''_{k3}	2.89	kA	Three-phase initial symmetrical short-circuit current
R/X	0.1	-	X/R ratio

Table II
Parameters of Transformer

Symbols	Values	Units	Descriptions
S_r	630	MVA	Rated apparent power
U_{rHV}	400	kV	Rated voltage of high voltage (HV) winding
U_{rLV}	332	kV	Rated voltage of low voltage (LV) winding
u_{k12}	19.48	%	Short-circuit impedance
u_{r12}	1.137	%	Resistive part of short-circuit impedance
P_{FE}	205	kW	Iron losses
i_0	0.102	%	No-load current
$f_{acHV/LV}$	0.5	-	u_k division between HV and LV windings
X_{air}	111	Ohm	Air-core reactance
B_{sat}	1.96	T	Saturated flux magnitude density
B_r	1.64	T	Rated flux magnitude density
	YNyn0	-	Vector group

Table III
Parameters of MMC converter

Symbols	Values	Units	Descriptions
L	53.9	mH	Inductance of each converter arm
C	50	μF	Aggregated capacitance of each converter arm

References

[1] L. He and C.-C. Liu, "Parameter identification with PMUs for instability detection in power systems with HVDC integrated offshore wind energy," *IEEE Transactions on Power Systems*, vol. 29, no.2, Mar. 2014.

[2] L. He, C.-C. Liu, A. Pitto, and D. Cirio, "Distance protection of AC grid with HVDC- connected offshore wind generators," *IEEE Transactions on Power Delivery*, vol. 29, no.2, Apr. 2014.

[3] K. Bell, D. Cirio, A.M. Denis, L. He, C.-C. Liu, C. Moreira, and P. Panciatici, "Economic and technical criteria for designing future offshore HVDC grids," *IEEE PES*: Innovative Smart Grid Technologies, Gothenburg, Sweden, 2010.

[4] WindEnergy Network – Communication hub for the wind energy industry, *www.windenergynetwork.co.uk*, Mar. 2015.

[5] N. Singh, and J. Carlsson, "Energization study of five-terminal multi-level HVDC converter station," *2013 IEEE PES General Meeting*, Vancouver, BC, Canada, Jul. 2013.

[6] J. Peralta, H. Saad, S. Dennetiere, J. Mahseredjian, and S. Nguefeu, "Detailed and averaged models for a 401-level MMC-HVDC system", *IEEE Transactions on Power Delivery*, vol. 27, no.3, Jul. 2012.

[7] K. Friedrich, "Modern HVDC PLUS application of VSC in modular multilevel converter topology," *2010 IEEE International Symposium on Industrial Electronics (ISIE)*, Bari, Italy, Jul. 2010.

[8] J. Martinez, and B. Mork, "Transformer modeling for low- and mid-Frequency transients – a review," *IEEE Transactions on Power Delivery*, vol. 20, no.2, Apr. 2005.

[9] L. He and R. Voelzke, "Effects of pre-insertion resistor on energization of compensated Lines," *2016 IEEE PES General Meeting*, Boston, MA, Jul. 2016.